PCP
PLANT & CELL PHYSIOLOGY

Regular Paper

3D Confocal Laser Scanning Microscopy for the Analysis of Chlorophyll Fluorescence Parameters of Chloroplasts in Intact Leaf Tissues

Kenji Omasa*, Atsumi Konishi, Hikaru Tamura and Fumiki Hosoi

Graduate School of Agricultural and Life Sciences, The University of Tokyo, 1-1-1 Yayoi, Bunkyo, Tokyo, 113-8675 Japan

We analyzed the chlorophyll fluorescence parameters in a 3D cellular arrangement in vivo by using a modified Nipkow disk-type confocal laser scanning microscope (CLSM). We first defined the 3D values of Φ_{PSII} (photochemical yield of PSII) and NPQ (non-photochemical quenching) in mesophyll, epidermal and guard cell chloroplasts from the leaf surface to several tens of microns in depth. We also used this CLSM method to analyze the relationships between actinic light intensity and the chlorophyll fluorescence parameters for Boston fern and broad bean leaf specimens. As the actinic light intensity increased, the mean Φ_{PSII} values decreased and the NPQ values increased in all chloroplasts of Boston fern and broad bean leaf. These values differed with cell type and species. The Boston fern chloroplasts had lower Φ_{PSII} values than the broad bean chloroplasts, and vice versa for the NPQ values. The Φ_{PSII} values of Boston fern chloroplasts decreased in the order mesophyll, epidermal and guard cell chloroplasts. The NPQ values decreased in the order guard cell, mesophyll and epidermal chloroplasts, except at 12 µmol m^{-2} s^{-1} actinic light, when the mesophyll value was slightly lower than that of the epidermis. The trend in the Φ_{PSII} and NPQ values of broad bean mesophyll and guard cell chloroplasts was opposite to that of Boston fern chloroplasts. As 3D CLSM can provide the Φ_{PSII} and NPQ values of each chloroplast in a 3D cellular arrangement, this method has potential for investigating differences in the functions of chloroplasts in vivo.

Keywords: 3D • Chlorophyll fluorescence • Chloroplast • CLSM • NPQ • Φ_{PSII}.

Abbreviations: 3D, three dimensional; *a*, absorption coefficient of photosynthetic pigments; A/D, analog to digital; CLSM, confocal laser scanning microscopy; ${}^{i}D_{t}$, dark current image integrated for *t* ms; EM-CCD, electron-multiplying charge-coupled device; ETR, electron transport rate; ${}^{i}F$, chlorophyll fluorescence intensity image measured under actinic light; ${}^{i}F_{m}$, chlorophyll fluorescence intensity image measured during a saturation light pulse in darkness; ${}^{i}F_{m}'$, chlorophyll fluorescence intensity image measured during the saturation light pulse under actinic light; *I*, irradiated light intensity; ND, neutral density; NPQ, non-photochemical quenching of chlorophyll fluorescence; PPF, photosynthetic photon flux; Q_A, primary quinone acceptor of PSII; Q_B, secondary quinone acceptor of PSII; R^2, coefficient of determination; ΦF, chlorophyll fluorescence yield under actinic light; ΦF_m, chlorophyll fluorescence yield during a saturation light pulse in the dark; $\Phi F_m'$, chlorophyll fluorescence yield during a saturation light pulse under actinic light; ΦF_0, minimum chlorophyll fluorescence yield after dark adaptation; ΦF_v, $\Phi F_m - \Phi F_0$,; $\Phi F_v/\Phi F_m$, maximum photochemical yield of PSII after dark adaptation; Φ_{PSII}, photochemical yield of PSII; λ, wavelength of light.

Introduction

Chlorophyll fluorescence imaging is one of the leading methods used to assess plant photosynthetic activities, because information is provided without the need for destruction of, or contact with, the living leaves (Omasa et al. 1987, Daley et al. 1989, Genty and Meyer 1995, Rolfe and Scholes 1995, Lichtenthaler and Miehe 1997, Govindjee and Nedbal 2000, Omasa and Takayama 2002, Osmond and Park 2002, Omasa and Takayama 2003, Papageorgiou and Govindjee 2004, Chaerle et al. 2007, Omasa et al. 2007). Chlorophyll fluorescence microscopy is an advanced imaging technique used to detect photosynthetic activity at the level of individual cells and chloroplasts in a non-invasive manner (Oxborough 2004). The first chlorophyll fluorescence microscopy technique was developed by Oxborough and Baker (1997a) and applied the 'saturation pulse method' for calculating Φ_{PSII},

*Corresponding author: Email, aomasa@mail.ecc.u-tokyo.ac.jp; Fax, +81-3-5841-8175.

Plant Cell Physiol. 50(1): 90–105 (2009) doi:10.1093/pcp/pcn174, available online at www.pcp.oxfordjournals.org

which represents the quantum yield of photosynthetic electron transport (Genty et al. 1989). This technique has since been used for applications that include comparing responses at the chloroplast level in mesophyll and guard cells with changes in ambient CO_2, O_2, light and humidity levels (Oxborough and Baker 1997a, Oxborough and Baker 1997b, Baker et al. 2001, Lawson et al. 2002, Lawson et al. 2003); investigating the effects of exposing leaf cells to ozone (Leipner et al. 2001); assessing the heterogeneity of cells and coenobia of microalgae (Küpper et al. 2000); and detecting herbicide stress in algae at different growth stages (Endo and Omasa 2004).

The generation of 3D information on the inherently complicated 3D structures of leaf tissues, cells and chloroplasts is required to improve our understanding of plant functioning and responses to stresses (Rigaut et al. 1992, Omasa 2000, Schurr et al. 2006, Omasa et al. 2007). In 3D surface microscopy of chlorophyll fluorescence, extended-focus Φ_{PSII} images of the leaf tissue surface were reconstructed from 39 images of chlorophyll fluorescence, taken at different focal planes at 5.5 µm intervals and with a 10× objective lens (Rolfe and Scholes 2002). Thereafter, the reconstruction of 3D cell-level Φ_{PSII} from <15 images taken at 4 µm intervals was achieved by using a modified shape-from-focus algorithm and higher magnification (×20) lens (Endo and Omasa 2007). Despite the highly efficient methods for reconstruction used by these two previous studies, the internal 3D anatomy of tissues and cells was not visualized, as the 3D surface reconstruction was performed passively. Furthermore, the objective magnifications were not sufficient to capture high-resolution images of chloroplasts within the cells.

Confocal laser scanning microscopy (CLSM), invented by Minsky (1988), is an active microscopic technique with the capacity for higher resolution and performance for 3D reconstruction than conventional passive light microscopy (Rigaut et al. 1992). This is because CLSM eliminates out-of-focus haze in objects by passing the excitation laser beam and the reflected or fluorescent light from the objects through pinholes (Nakano 2002). CLSM can also reconstruct images of the internal 3D anatomy of tissues and cells by capturing the fluorescence from fluorochromes within the tissues and cells. These advantages have enabled the use of CLSM for chlorophyll fluorescence microscopy of leaf tissue profiles (Osmond et al. 1999) and of chloroplast movement in vivo (Tlałka and Fricker 1999, Tlałka et al. 1999). One disadvantage of the galvanometer-mirror-type CLSM approach is the requirement for specimens to be irradiated with a strong excitation laser beam in order to capture clear images; the use of this galvanometer-mirror makes it technically difficult to scan and evenly irradiate specimens rapidly (Wang et al. 2005). These issues prevent the use of the saturation pulse method with CLSM for obtaining the Φ_{PSII} and NPQ chlorophyll fluorescence parameters. Recent advances in high-speed rotating pinhole disk (Nipkow disk) CLSM (Ichihara et al. 1996, Tanaami et al. 2002) and highly sensitive cooled electron-multiplying charge-coupled device (EM-CCD) technologies have made it possible to scan rapidly, evenly irradiate and capture clear internal fluorescence images of a specimen under a low-intensity laser beam that has approximately 1/1,000 the intensity of the galvanometer-mirror-type laser beam. The large number of confocal pinholes in the high-speed rotating disk makes it possible to use this lower intensity beam. Recently, we developed a novel computer-aided CLSM system for applying the saturation pulse method through a modification of the Nipkow disk CLSM and the use of a high sensitivity EM-CCD camera (Omasa and Konishi 2008). This system can be used to analyze the internal 3D anatomy of leaf tissues and cells and to assess differences in chlorophyll fluorescence parameters in vivo for each chloroplast at the ordinary range of actinic light intensity, using objectives >40×. In our previous study we did not apply the system to the estimation of Φ_{PSII} and NPQ chlorophyll fluorescence parameters, so the performance of the system was not assessed. For this reason, in our current study, we investigated the performance of this system and assessed differences in the chlorophyll fluorescence parameters of epidermal, guard cell and mesophyll chloroplasts in reconstructed 3D images of Boston fern (*Nephrolepis exaltata* L. 'Bostoniensis') and broad bean (*Vicia faba* L. 'Komasakae') leaf specimens under different actinic light intensities.

Results

Confirmation of saturation light pulse intensity and duration of saturation of photosynthetic electron transport

We examined the relationships between the intensity [photosynthetic photon flux (PPF)] of the light pulse falling on the Boston fern leaf and the chlorophyll fluorescence yields of mesophyll and guard cell chloroplasts, as measured from the abaxial leaf surface by the CLSM system, and the tissue-level yields at the abaxial leaf surface, as measured with a conventional chlorophyll fluorescence imaging system (see Materials and Methods, Omasa and Takayama 2003) (**Fig. 1**). **Fig. 1A** and **B** shows the results for a dark-adapted leaf and a leaf adapted under light of 300 µmol m^{-2} s^{-1} PPF, respectively. The chlorophyll fluorescence yield (ratio) on the vertical axis is the ratio of chlorophyll fluorescence intensity at each PPF to the average saturated intesnity. The fluorescence yields of the dark-adapted leaf increased dramatically with a slight increase in light intensity, reaching approximately 1.0 at a PPF of 800 µmol m^{-2} s^{-1} (dotted line in **Fig. 1A**). The fluorescence yields of the light-adapted leaf increased more gradually than those of the dark-adapted leaf, reaching approximately 1.0 at a PPF of 1,300 µmol m^{-2} s^{-1} (dotted line in **Fig. 1B**). The same trends were observed in the changes in

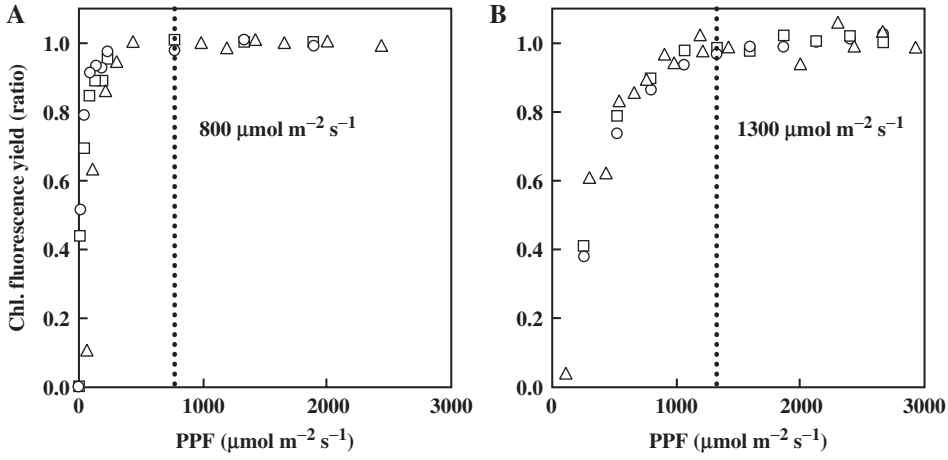

Fig. 1 Relationships between light pulse intensity (PPF) and chlorophyll fluorescence yields of mesophyll and guard cell chloroplasts of Boston fern leaf specimens (as measured from the abaxial leaf side with the CLSM system) and chlorophyll fluorescence yield of the abaxial leaf surface (as measured with a conventional chlorophyll fluorescence imaging system). (A) Results in the dark. (B) Results in 300 μmol m^{-2} s^{-1} actinic light. Open squares, circles and triangles represent chlorophyll fluorescence yields of mesophyll chloroplasts, guard cell chloroplasts and the abaxial leaf surface, respectively. The yield values were the averages of 20 chloroplasts for mesophyll cells and 10 chloroplasts for guard cell chloroplasts. Dotted lines represent the minimal PPF for the saturation light pulse.

the fluorescence yield of mesophyll and guard cell chloroplasts, as measured with the CLSM system, and in the tissue-level yields of the abaxial leaf surface, as measured with the conventional imaging system.

We measured the chlorophyll fluorescence transients of Boston fern mesophyll chloroplasts from the abaxial leaf side with the CLSM system under different saturation light intensities (**Fig. 2**). **Fig.2a, b** and **c** shows the results for leaves acclimatized to actinic light at 248, 98 and 0 μmol m^{-2} s^{-1}, respectively. The saturation light intensity was 4,820 μmol m^{-2} s^{-1} in 0 μmol m^{-2} s^{-1} actinic light and 24.33 times the actinic light intensity in 248 and 98 μmol m^{-2} s^{-1} actinic light. The arrows indicate the duration of saturation, at >97% of the maximum intensity, in each transient. The fluorescence intensity increased rapidly after irradiation under the saturation light intensity and reached 97% of the maximum intensity in 0.12 s under actinic light at 248 and 98 μmol m^{-2} s^{-1} and in 0.15 s under actinic light at 0 μmol m^{-2} s^{-1}. The duration of saturation ranged from 2.2 to 2.9 s, with the largest duration associated with the highest intensity of actinic light. We reconstructed a 3D image by capturing a series of chlorophyll fluorescence intensity images during the saturation laser light pulse in the dark and light in 64 different focal planes for 1.92 s from 0.2 s after the start of irradiation.

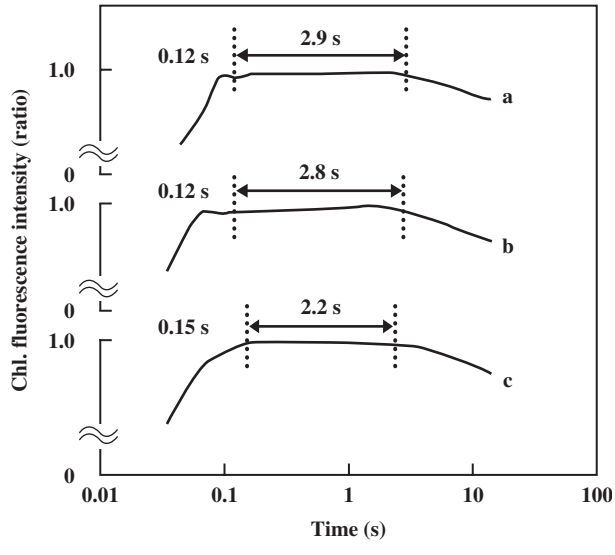

Fig. 2 Chlorophyll fluorescence transients of mesophyll chloroplasts of Boston fern leaf specimens, as measured from the abaxial leaf side with the CLSM system under different saturation light intensities. The chlorophyll fluorescence intensity was the average of 20 mesophyll chloroplasts. a, b and c represent the results for leaves acclimatized to 248, 98 and 0 μmol m^{-2} s^{-1} actinic light PPF, respectively. The saturation light was 4,820 μmol m^{-2} s^{-1} PPF in 0 μmol m^{-2} s^{-1} actinic light and 24.33 times the actinic light in 248 and 98 μmol m^{-2} s^{-1} actinic light PPF. Durations from the peak intensities to 97% of the peak intensities are indicated by arrows wedged between dotted lines.

Reconstruction of 3D chlorophyll fluorescence intensity images and calculation of chlorophyll fluorescence parameters

We examined three chlorophyll fluorescence intensity images of a Boston fern leaf specimen selected from a series of images captured in 64 different focal planes during irradiation for approximately 2 s with a saturation light pulse of 4,820 μmol m^{-2} s^{-1} PPF (**Fig. 3A**). We also examined 3D images

reconstructed from the 64 planes before 3D deconvolution (**Fig. 3B**), and the images after 3D deconvolution (**Fig. 3C**). **Fig. 3D** is a transmitted light image of the same microscopic abaxial leaf area. In samples of A(*i*), *i* = 10, 30 and 50, where '*i*' is the order of focal planes with different *z* coordinates at increasing depth from the abaxial leaf surface to the inside of the leaf. As the *z*-scan interval was 1.25 µm, A(10), A(30) and A(50) were at focal plane depths of 12.5, 37.5 and 62.5 µm, respectively, from the leaf surface. The distance from the leaf surface to A(64) was 80 µm. Focused and defocused fluorescence areas are apparent in **Fig. 3A**. In A(10), fluorescent chloroplasts in guard cells appear at the center of the image. Some brightly fluorescent chloroplasts in the epidermal cells are also apparent. In A(30), the guard cell chloroplasts are not apparent and a large number of fluorescent mesophyll chloroplasts are found, especially along the boundaries of the cells. In A(50), a number of fluorescent chloroplasts are found on the right side of the focal plane. Spike noises in all focal planes were first eliminated by applying a median filter with a mask size of 3 × 3 pixels.

The 3D chlorophyll fluorescence intensity images were reconstructed by building the acquired planes. **Fig. 3B** is a reconstructed 3D image from the abaxial surface and the side. The configuration of the fluorescent chloroplasts in the reconstructed 3D images reflected the configuration normally observed in vivo. The reconstructed images were then deconvoluted to obtain a clearer configuration (**Fig. 3C**). The deconvolution image was clearer, but the analog to digital (A/D) conversion level of the chlorophyll fluorescence intensity was inaccurate. Therefore, we used the reconstructed images before the deconvolution to calculate the Φ_{PSII} and NPQ values, and used the deconvolution image to produce a 1-bit binary image to extract only the chloroplast images (see Materials and Methods). **Fig. 3D** is a transmitted

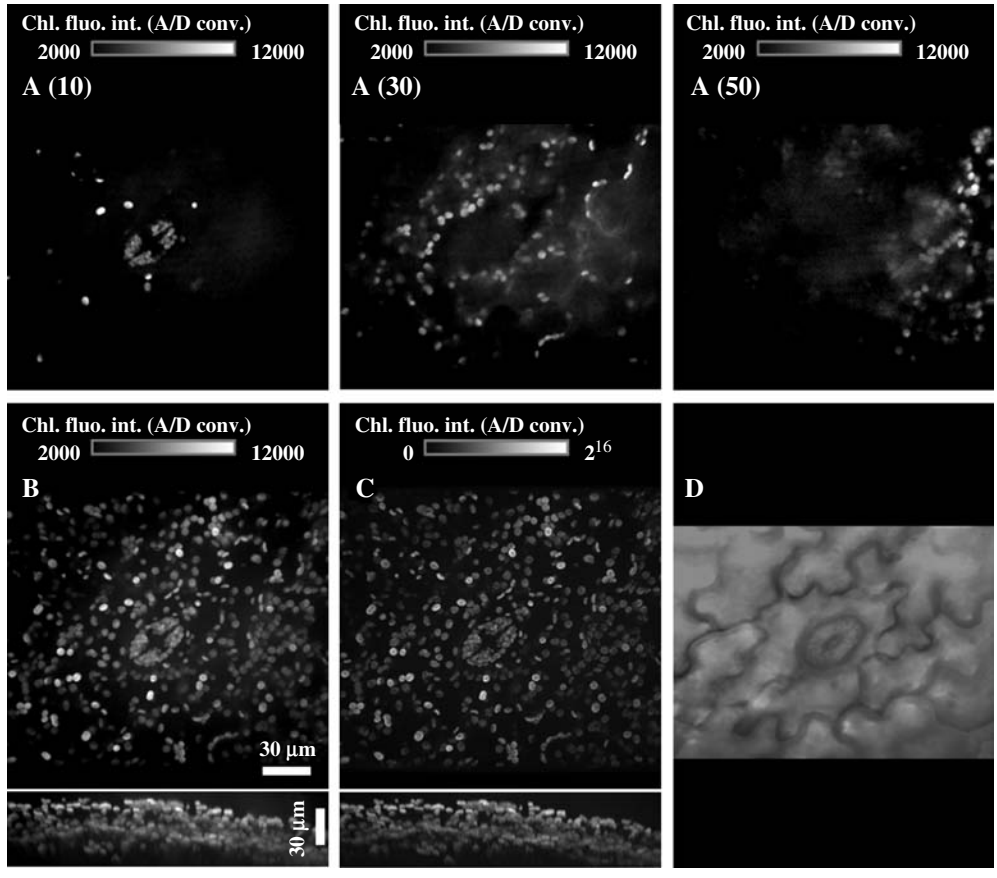

Fig. 3 (A) Chlorophyll fluorescence intensity images of Boston fern leaf specimen, selected from a series of images captured at 64 different focal planes (= different *z* coordinates) during irradiation for approximately 2 s with a saturation light pulse. The value in parentheses for each image in A (10, 30, 50) is the number of the focal plane from the abaxial leaf surface to the inside of the leaf. The saturation light pulse was 4,820 µmol m^{-2} s^{-1} PPF. (B) 3D images reconstructed from the 64 planes before 3D deconvolution. (C) 3D deconvoluted images. (D) Transmitted light image of the same microscopic abaxial leaf area. The images from the surface and profile are shown in B and C.

light image of the same region in B and C captured with a color CCD camera. A stoma is at the center of the image, and the epidermal cells have intricate shapes. Epidermal cell chloroplasts emitted more intense fluorescence than the mesophyll or guard cell chloroplasts (**Fig. 3B, C**). The guard cell chloroplasts were smaller and denser than the mesophyll chloroplasts. The inclination of the leaf to the right is apparent in the profile image (**Fig. 3B, C**).

After the reconstructed 3D chlorophyll fluorescence intensity images were processed by affine transformation to adjust the position gap between the images and to extract only the chloroplasts images, the chlorophyll fluorescence yields and parameters such as Φ_{PSII} and NPQ were calculated by Equations (1)–(5) (see Materials and Methods). **Fig. 4** shows close-up 3D images of ΦF, $\Phi F_m'$ and Φ_{PSII} reconstructed from a series of chlorophyll fluorescence intensity images captured under 198 µmol m^{-2} s^{-1} PPF actinic light and 4,820 µmol m^{-2} s^{-1} PPF saturation pulse; the images were taken at the same site shown in **Fig. 3**. Profile images were reconstructed for the areas surrounded by the red and the sky-blue dotted lines (**Fig. 4A**) and are shown at the bottom and the right side, respectively, of the abaxial surface image. Epidermal cell chloroplasts had larger ΦF and $\Phi F_m'$ values than guard cell and mesophyll chloroplasts. The Φ_{PSII} values of the epidermal cell chloroplasts and the guard cell chloroplasts were lower than those of the subjacent mesophyll chloroplasts. 3D-ΦF, 3D-$\Phi F_m'$ and 3D-Φ_{PSII} images were reconstructed clearly, because there was very little movement of all the chloroplasts during the capture of ^iF and $^iF_m'$ images, but accurate 3D-NPQ images were not reconstructed, because there was movement of some of the chloroplasts—especially the mesophyll chloroplasts—during the gap of several tens of minutes between the captures of ^iF_m and $^iF_m'$.

Relationships between actinic light intensity and chlorophyll fluorescence parameters of chloroplasts in mesophyll cells, guard cells and epidermal cells

We examined the relationships between actinic light intensity and the chlorophyll fluorescence parameters Φ_{PSII} and NPQ for the Boston fern and broad bean chloroplasts on the abaxial leaf side. As the actinic light intensity increased, Φ_{PSII} decreased and NPQ increased in all mesophyll, guard cell and epidermal chloroplasts of Boston fern and broad bean leaf specimens. The Φ_{PSII} values were lower for Boston fern chloroplasts than for broad bean chloroplasts, and vice versa for the NPQ values (**Fig. 5**). The maximum photochemical yield of PSII, $\Phi F_v/\Phi F_m$, for attached mature leaves on the abaxial side, measured with a pulse amplitude modulation (PAM) 101 fluorimeter, was approximately 0.55 for Boston fern plants and approximately 0.65 for broad bean plants. These $\Phi F_v/\Phi F_m$ values were similar to the mean Φ_{PSII} values for mesophyll chloroplasts at 12 µmol m^{-2} s^{-1} actinic light. There was no bleaching of leaf specimens during the experiments.

For Boston fern leaf specimens, the mean Φ_{PSII} values of mesophyll, epidermal and guard cell chloroplasts decreased from 0.52 to 0.16, from 0.42 to 0.11 and from 0.34 to 0.09, respectively, with increasing actinic light intensity (**Fig. 5A**). The Φ_{PSII} values of the mesophyll chloroplasts were larger than those of the epidermal and guard cell chloroplasts at all actinic light intensities. The Φ_{PSII} values of epidermal chloroplasts were larger than those of the guard cell chloroplasts at all actinic light intensities. The mean NPQ values of mesophyll, epidermal and guard cell chloroplasts increased from 0.20 to 1.81, from 0.34 to 1.56 and from 0.36 to 1.94, respectively, with increasing actinic light intensity (**Fig. 5B**). The NPQ values of the guard cell chloroplasts were larger than

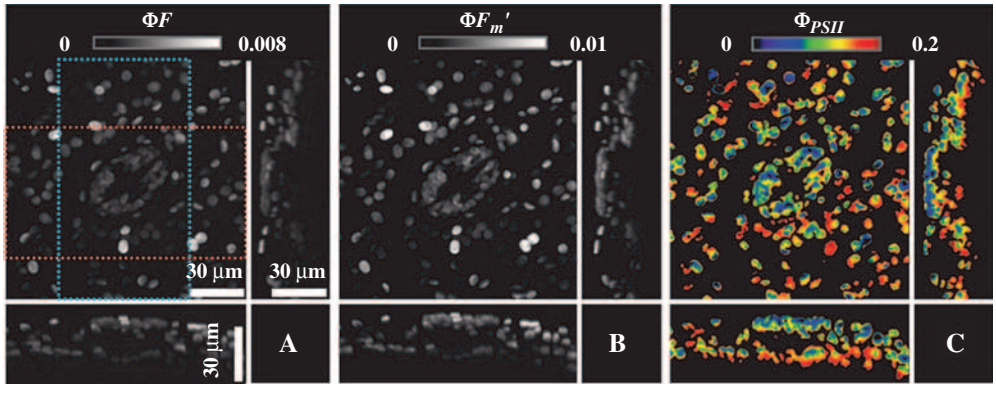

Fig. 4 Close-up 3D images of ΦF, $\Phi F_m'$ and Φ_{PSII} reconstructed from a series of chlorophyll fluorescence intensity images captured at the same site shown in **Fig. 3** under 198 µmol m^{-2} s^{-1} PPF actinic light and a saturation light pulse of 4,820 µmol m^{-2} s^{-1} PPF. (A) ΦF; (B) $\Phi F_m'$; (C) Φ_{PSII}. Profile images were reconstructed in the areas surrounded by the red and the blue dotted lines (A) and are shown at the bottom and the right side, respectively, of the abaxial surface image.

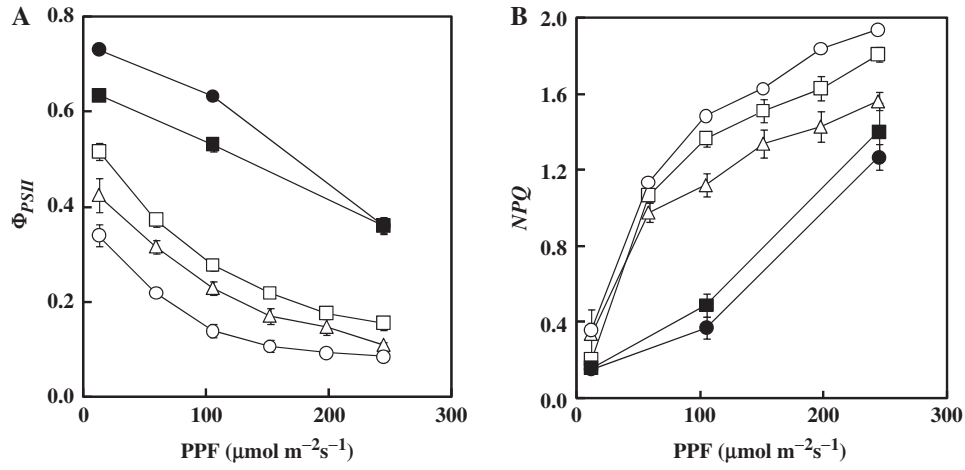

Fig. 5 Relationships between actinic light intensity (PPF) and the chlorophyll fluorescence parameters (A) Φ_{PSII} and (B) NPQ. Open squares, triangles and circles represent the values for the subjacent mesophyll chloroplasts, epidermal chloroplasts and guard cell chloroplasts on the abaxial side, respectively, of Boston fern leaf specimens. Filled squares and circles represent the values for the subjacent mesophyll chloroplasts and guard cell chloroplasts on the abaxial side, respectively, of broad bean leaf specimens. The Φ_{PSII} and NPQ values were the averages for 16 chloroplasts, and the vertical bars represent the standard errors ($n = 16$), except in the case of Boston fern epidermal cells irradiated with 12 μmol m^{-2} actinic light, for which the average values were calculated for eight chloroplasts ($n = 8$).

those of the mesophyll and epidermal chloroplasts at all actinic light intensities. The NPQ values of the mesophyll chloroplasts were larger than those of the epidermal chloroplasts. The exception was at 12 μmol m^{-2} s^{-1} actinic light; at this PPF, the mesophyll value was slightly lower than that of the epidermis.

For broad bean leaf specimens, the mean Φ_{PSII} values of mesophyll chloroplasts and guard cell chloroplasts decreased from 0.63 to 0.36 and from 0.73 to 0.36, respectively, with increasing actinic light intensity (**Fig. 5A**). The Φ_{PSII} values of the mesophyll chloroplasts were lower than those of the guard cell chloroplasts at all actinic light intensities. The mean NPQ values of mesophyll chloroplasts and guard cell chloroplasts increased from 0.16 to 1.40 and from 0.15 to 1.27, respectively, with increasing actinic light intensity (**Fig. 5B**). The NPQ values of the mesophyll chloroplasts were larger than those of the guard cell chloroplasts at all actinic light intensities. Epidermal chloroplasts were not found in the broad bean leaf specimens. The Φ_{PSII} and NPQ values of broad bean mesophyll and guard cell chloroplasts showed the opposite trend to the equivalent chloroplasts in Boston fern specimens.

The value obtained by multiplying the PPF value of actinic light by the Φ_{PSII} value is an indicator of photosynthetic electron transport rate (ETR) and CO_2 fixation rate. We therefore examined the relationship between actinic light intensity (PPF) and $\Phi_{PSII} \times$ PPF values (**Fig. 6**). For Boston fern leaf specimens, the $\Phi_{PSII} \times$PPF values of mesophyll, epidermal and guard cell chloroplasts increased from 6.3 to 38 μmol m^{-2} s^{-1}, from 5.2 to 27 μmol m^{-2} s^{-1} and from 4.2 to

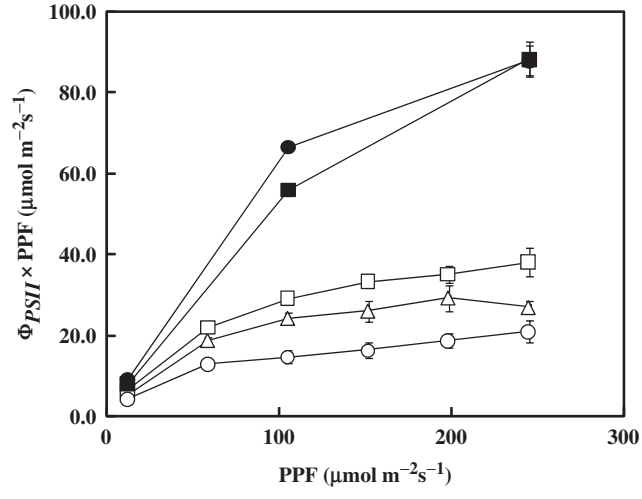

Fig. 6 Relationships between actinic light intensity (PPF) and $\Phi_{PSII} \times$ PPF values obtained from data in **Fig. 5**. The symbols correspond to those shown in **Fig. 5**. The vertical bars represent the standard errors.

21 μmol m^{-2} s^{-1}, respectively, with increasing actinic light intensity. For broad bean leaf specimens, the $\Phi_{PSII} \times$ PPF values of mesophyll and guard cell chloroplasts increased from 7.8 to 88 μmol m^{-2} s^{-1} and from 8.9 to 88 μmol m^{-2} s^{-1}, respectively. These results indicate that the increases in ETR and CO_2 fixation rates of Boston fern chloroplasts are lower than those of broad bean chloroplasts. In addition, the initial increase in these rates was larger in the order mesophyll, epidermal and guard cell chloroplasts in Boston fern specimens

and in the order guard cell and mesophyll chloroplasts in broad bean specimens.

We also examined the relationships between the Φ_{PSII} and NPQ values of mesophyll chloroplasts and the Φ_{PSII} and NPQ values of epidermal and guard cell chloroplasts (**Figs. 7, 8**). We found rough correlations, related to the equation $y = x$, between the Φ_{PSII} and NPQ values of mesophyll chloroplasts and the values of epidermal and guard cell chloroplasts. Changes in Φ_{PSII} values from mesophyll chloroplasts were −0.03 to −0.09 (−15 to −30%) for Boston fern epidermal chloroplasts, −0.07 to −0.18 (−34 to −51%) for Boston fern guard cell chloroplasts and 0.00 to 0.10 (0 to 19%) for broad bean guard cell chloroplasts. In comparison, the changes in NPQ values from mesophyll chloroplasts were −0.25 to 0.14 (67 to −18%) for Boston fern epidermal chloroplasts, 0.07 to 0.21 (7 to 77%) for Boston fern guard cell chloroplasts and −0.01 to −0.13 (−5 to −24%) for broad bean guard cell chloroplasts.

Discussion

Performance of the new CLSM system for application of the saturation pulse method

The saturation pulse method has been proposed as a powerful tool for assessing photosynthetic parameters (Genty et al. 1989, Bilger and Björkman 1990, Schreiber 2004). Application of the saturation pulse method using the CLSM system requires measurement of the laser beam intensity on the specimen. However, the diameter of the laser beam as viewed through the objective lens focused on the specimen is much smaller than the measuring face of the PPF sensor. We addressed this problem by developing a method for converting the laser beam focused on the measuring plane via an objective lens to PPF by using a PPF sensor and a metal pinhole disk 50 μm in diameter (see Materials and Methods). In these experiments, laser power (mW) was converted to PPF (μmol m^{-2} s^{-1}) by the equation PPF = 11,311 × laser power − 833.4. The equation revealed that the PPF of the CLSM at maximum laser power (23.0 mW) for chlorophyll fluorescence measurements was extremely strong at approximately 260,000 μmol m^{-2} s^{-1}.

The light intensity changes were controlled with two electromagnetic shutters installed in the system. The intensity was maintained at the dark or actinic light value and had the capacity to change rapidly from dark or actinic light intensity to saturation light pulse intensity and then back again. The time taken to maximize the light intensity of the system was approximately 0.12–0.15 s (see **Fig. 2**), and the intensity was minimized within 0.27 s. These are faster than the equivalent times taken by commercially available PAM chlorophyll fluorometers (e.g. WALZ, MINI-PAM and PAM-101).

In previous imaging studies of laser-induced chlorophyll fluorescence transients (Omasa 1998, Omasa and Takayama 2002), the laser beam irradiations pulsed with a scan frequency of 30 s^{-1}; this was because PPF averages of 50–200 μmol m^{-2} s^{-1} caused transients similar to those of a continuous xenon lamp. In comparison, the laser scan frequency of our rotating pinhole- (Nikpow disk) type CLSM system was from 300 to 360 s^{-1}, which is 10–12 times the frequency obtained in previous studies. For this reason, we concluded that the pulse of the laser beam had no effect on the photochemical or non-photochemical activity measured by the chlorophyll fluorescence. The fluctuations in laser beam intensity measured every 30 ms by the EM-CCD camera were very small (actinic light, ±1.5% and saturation light pulse, ±0.45%, see **Supplementary Fig. A**). Consequently, the pulsed laser beam irradiated with the rotating

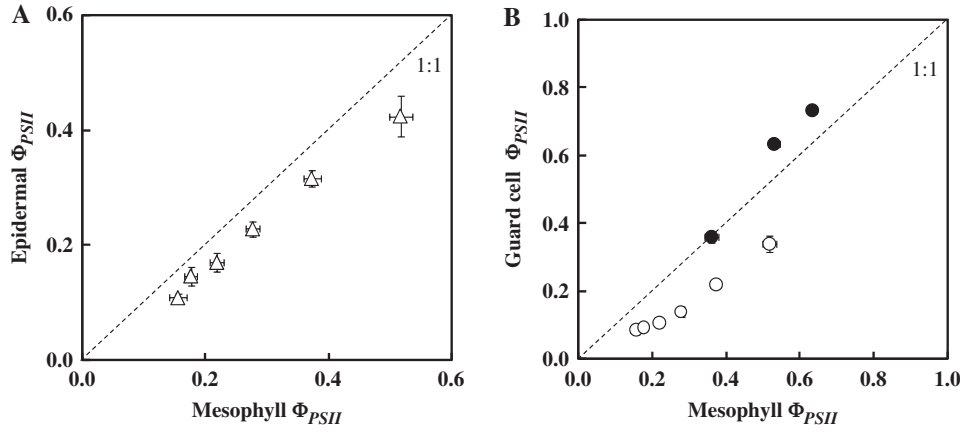

Fig. 7 Relationships between Φ_{PSII} values of mesophyll chloroplasts and those of epidermal cell and guard cell chloroplasts, obtained from data in **Fig. 5A**. (A) Relationship between Φ_{PSII} values of mesophyll and epidermal chloroplasts. (B) Relationship between Φ_{PSII} values of mesophyll and guard cell chloroplasts. The symbols correspond to those shown in **Fig. 5**. The vertical and horizontal bars represent the standard errors.

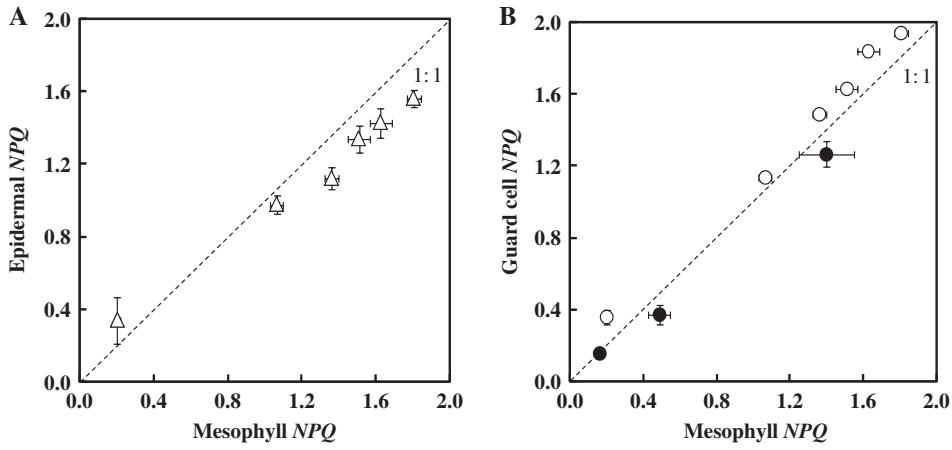

Fig. 8 Relationships between NPQ values of mesophyll chloroplasts and those of epidermal cell and guard cell chloroplasts, obtained from data in **Fig. 5B**. (A) Relationship between NPQ values of mesophyll and epidermal chloroplasts. (B) Relationship between NPQ values of mesophyll and guard cell chloroplasts. The symbols correspond to those shown in **Fig. 5**. The vertical and horizontal bars represent the standard errors.

pinhole Nipkow disk could be used to supply actinic light and saturation pulses to the plants.

The saturation pulse intensity required to saturate photosynthetic electron transport differed with the intensity of actinic light. A saturation pulse of >800 μmol m^{-2} s^{-1} in the dark and 1,300 μmol m^{-2} s^{-1} under 300 μmol m^{-2} s^{-1} actinic light was sufficient to saturate the photosynthetic electron transport in mesophyll and guard cell chloroplasts in the abaxial leaf surfaces of Boston fern specimens (**Fig. 1**). This is because adequately photoactivated PSII requires stronger light; the excess light energy is dissipated as heat (Bilger and Björkman 1990, Noctor and Horton 1990). Furthermore, as demonstrated in **Fig. 1**, the consistent trends obtained by the modified CLSM system and the conventional system for the relationships between chlorophyll fluorescence yield and PPF values and in the minimum intensities required to saturate the photosynthetic electron transport validated our estimations of laser beam intensity.

Imaging of ubiquitous chloroplasts in leaf tissues under high-resolution objectives requires the reconstruction of clear 3D images from the many images captured at different focal planes. Our modified CLSM system has made it possible to reconstruct the 3D images, even when the objective is ×40 and the leaf tissue was inclined (**Fig. 3**). The precise reconstruction of 3D images requires at least 64 focal planes, especially when 3D deconvolution is applied. To calculate Φ_{PSII} and NPQ it is necessary to capture ${}^{i}F_m$ and ${}^{i}F_m'$ images while the photosynthetic electron transport is saturated; we therefore examined the saturation duration of the photosynthetic electron transport of PSII. Chlorophyll fluorescence intensities peak as electron acceptors such as Q_A (the primary quinone acceptor after PSII), Q_B (the secondary quinone acceptor after PSII) and plastoquinone are reduced; thereafter, quenching occurs under continual light (Lazár 1999, Strasser et al, 2004). The time taken to reach photochemical saturation was longer in dark-adapted leaves than that in light-adapted leaves. This result implies that it took longer to reduce fully Q_A that had been adequately oxidized in the dark than Q_A that had already been reduced by actinic light (**Fig. 2**). Saturation duration was longer in the light than in the dark. Heat dissipation may have been increased by acclimatization to light; therefore, the saturation light did not cause as rapid a change in ΔpH through the thylakoid membranes as would have occurred in the dark (Gilmore et al. 1998, Kramer et al. 1999, Krause and Jahns 2004). The fluorescence intensity peaked within 0.2 s after initiation of saturation light pulse irradiation and remained at a maximum level for at least 2.2 s (**Fig. 2**). The piezo z-scan unit installed on the objective made it possible to capture the image from each different focal plane at 30 ms. It was possible to capture 64 images of ${}^{i}F_m$ or ${}^{i}F_m'$ for 3D reconstruction at different focal planes during the 1.92 s saturation period. The saturation light pulse did not cause photoinhibition and depress the photochemical yield of PSII, even at the highest light intensity of 6,180 μmol m^{-2} s^{-1} for 3.5 s (see **Supplementary Fig. B**). The focal planes for reconstructing the 3D-${}^{i}F$ image were captured under actinic light at an exposure time of 700–1,000 ms, or 3000 ms with a PPF of 12 μmol m^{-2} s^{-1}, without changing the EM-CCD camera digital gain values from those used for capturing the ${}^{i}F_m$ and ${}^{i}F_m'$ images. The 64 focal planes were captured in 44.8–64 s, or 192 s with a PPF of 12 μmol m^{-2} s^{-1}. The relatively long exposure time was possible because of the steady-state fluorescence intensity conditions that occurred under the actinic light.

Photosynthetic properties of chloroplasts in mesophyll cells, guard cells and epidermal cells

Chlorophyll fluorescence intensity images of leaf tissue cross-section surfaces reveal the light distribution within the leaf (Takahashi et al. 1994, Koizumi et al. 1998, Han et al. 1999, Osmond et al. 1999, Pfündel and Neubohn 1999, Vogelmann and Evans 2002, Evans and Vogelmann 2003). In comparison, the new CLSM system makes it possible to capture profile images at a much higher resolution without the need for leaf cross-sections, although the depth is limited to within 100 µm. The abaxial profile images captured from Boston fern leaf specimens (**Fig. 3**) suggest that there are bright chloroplasts near the leaf surface—especially epidermal chloroplasts, which were exposed to stronger light than were the subjacent mesophyll chloroplasts. The high density of chloroplasts near the cell boundaries implies that large numbers of chloroplasts are required near intercellular spaces to allow efficient CO_2 fixation (Evans and von Caemmerer 1996).

With increasing actinic light intensity, the mean values of Φ_{PSII} decreased and the mean values of NPQ increased in the subjacent mesophyll, guard cell and epidermal chloroplasts (**Fig. 5**). This trend was observed because the photosynthetic efficiency decreases as a result of the increase in heat dissipation that occurs under strong light conditions (Goh et al. 1999, Lawson et al. 2002, Lawson et al. 2003). As another reason for this trend, there might be a deficiency in the supply of CO_2 for photosynthesis by chloroplasts in the cells with increasing actinic light intensity (Terashima et al. 2001, Lowson et al. 2002). In addition, the abaxial leaf surface (with stomata) touching the cover glass was in water and the adaxial leaf surface (without stomata) was in air, thus decreasing the CO_2 supply to the chloroplasts. The mean values of Φ_{PSII} and NPQ varied between species and cell type (**Fig. 5**). At all actinic light intensities the Φ_{PSII} values were lower for Boston fern chloroplasts than for broad bean chloroplasts, and vice versa for NPQ values. The Φ_{PSII} and NPQ values of Boston fern chloroplasts changed largely in response to a light intensity increase at low light intensity, whereas the values for broad bean chloroplasts did not. The Φ_{PSII} values of Boston fern chloroplasts decreased in the order subjacent mesophyll, epidermal and guard cell chloroplasts, and the NPQ values decreased in the order guard cell, subjacent mesophyll and epidermal chloroplasts, except at 12 µmol m^{-2} s^{-1} actinic light, when the NPQ value for mesophyll chloroplasts was just lower than that for epidermal chloroplasts. The Φ_{PSII} and NPQ values of broad been mesophyll and guard cell chloroplasts showed a trend opposite to those of Boston fern chloroplasts. The Φ_{PSII} × actinic light PPF value, as an indicator of the photosynthetic ETR and CO_2 fixation rate, increased with increasing actinic light intensity (**Fig. 6**). However, the rates for Boston fern chloroplasts did not exceed half the rates observed for broad bean chloroplasts, and the increased rates were a little above 50 µmol m^{-2} s^{-1} actinic light.

The Φ_{PSII} values of guard cell chloroplasts have been previously reported to be indistinguishable from, or only slightly lower (minimum of 79%) than, those of mesophyll chloroplasts (Baker et al. 2001) according to the variety of plant (Lawson et al. 2002, Lawson et al. 2003). In general, our results support this tendency (see **Fig. 7**). However, the light intensity was attenuated in the leaf tissue; therefore, the overlying chloroplasts were irradiated by stronger light than the underlying chloroplasts. Consequently, if the chloroplasts are of the same quality, the Φ_{PSII} values should be lower and NPQ values higher in the overlying chloroplasts than in the underlying chloroplasts. This trend was observed for Φ_{PSII} profiles (**Fig. 3**).

Our calculated Φ_{PSII} values for chloroplasts of Boston fern leaves with lower $\Phi F_v/\Phi F_m$ (=0.55) value were lower than those generally known in higher plants (Lawson et al. 2002, Lawson et al. 2003). This might have been the result of inefficiency of photosynthetic electron transport in the ferns or a severe deficiency in the supply of CO_2 for photosynthesis by chloroplasts in the cells (Terashima et al. 2001, Lawson et al. 2002), because there were no stomata in the adaxial leaf surface exposed to air, and the abaxial leaf surface (with stomata) touched the cover glass wetted with water. The lower Φ_{PSII} × actinic light PPF values for Boston fern chloroplasts also suggest depression of the photosynthetic ETR and CO_2 fixation rate, although this indicator is influenced by the proportion of incident photons absorbed by PSII and other metabolic processes such as photorespiration, O_2 (through the Mehler reaction) and nitrate assimilation (Baker and Oxborough 2004). The Φ_{PSII} values for Boston fern guard cell chloroplasts were lower than the equivalent values observed for mesophyll chloroplasts: the differences were −0.07 to −0.18 (−34 to −51%)—larger than those reported for *Polypodium vulgare* and *Tradescantia albifora* by Lawson et al. (2003). Boston ferns have a greater number of small chloroplasts in their guard cells than do other higher plants (**Figs. 3, 4**); this may increase light absorption capacity and reduce PSII operating efficiency (Lawson et al. 2003). These findings may explain the higher NPQ values observed for guard cell chloroplasts than for mesophyll chloroplasts in the Boston fern (**Figs. 5B, 8**). Furthermore, the PSII operating efficiency was lower for the guard cell chloroplasts than for the adjacent mesophyll chloroplasts (Baker et al. 2001), and also for the mesophyll chloroplasts far away from the guard cells (**Fig. 4**).

The Φ_{PSII} values were slightly higher (the maximum is 19%) for guard cell chloroplasts of broad bean leaves with the normal $\Phi F_v/\Phi F_m$ value of 0.65 than for mesophyll chloroplasts, especially at low actinic light intensity. These results are consistent with those of previous reports, which found that the photosynthetic O_2 evolution rate is higher in broad

bean guard cells than in mesophyll cells (Shimazaki et al. 1982, Shimazaki 1989). In comparison, these findings do not agree with those reported by Lawson et al. (2003). It is likely that the energy for opening the stomata is provided mainly by the mitochondria and partly by the chloroplasts, although the energy source may vary with the prevailing environment (Shimazaki et al. 1983, Vani and Raghavendra 1994, Shimazaki et al. 2007) in higher plants, and the activity of ribulose bisphosphate carboxylase is lower in guard cell chloroplasts than in mesophyll chloroplasts (Kopka et al. 1997, Vavasseur and Raghavendra 2005). The high Φ_{PSII} values of broad bean guard cell chloroplasts may be related to the supply of ATP and NADH required for the opening of stomata.

Inhibition of photosynthetic electron transport from PSII to the cytochrome b_6/f complex (e.g. by the action of DCMU) causes an increase in chlorophyll fluorescence intensity (Govindjee 1995). In contrast, Φ_{PSII} and NPQ decrease owing to the disappearance of non-photochemical quenching (Govindjee and Seufferheld, 2002) caused by gradients of pH through thylakoid membranes (Gilmore et al. 1998, Kramer et al. 1999, Krause and Jahns 2004). The chlorophyll fluorescence intensities were higher for Boston fern epidermal chloroplasts than for mesophyll chloroplasts, whereas the Φ_{PSII} and NPQ values were lower (**Figs. 7, 8**). The differences in Φ_{PSII} of epidermal chloroplasts compared with that of mesophyll chloroplasts ranged from −0.03 to −0.09 (−15 to −30%); these differences were smaller than those observed between guard cell chloroplasts and mesophyll chloroplasts. These results suggest that photosynthetic electron transport is inherently or extrinsically more inefficient in epidermal chloroplasts than in mesophyll chloroplasts. Both Φ_{PSII} and NPQ are depressed when chronic photoinhibition occurs (Osmond et al. 1994). The epidermal chloroplasts are closer to the outside of the leaf than are the mesophyll chloroplasts; therefore, the former might have been subjected to stronger light than the latter. Consequently, chronic photoinhibition might have occurred in the epidermal chloroplasts in response to the strong light.

Materials and Methods

Plant material

Boston fern (*N. exaltata* L. 'Bostoniensis') plants were acclimatized in pots (10 cm diameter and 10 cm high) in an environmentally controlled growth chamber for 4 weeks before the experiments. The pots were filled with artificial soil (mixture of vermiculite and perlite, 2 : 1, v/v). The plants were illuminated for 12 h each day with fluorescent lights at a PPF of 150 µmol m^{-2} s^{-1}. Air temperature was 24.5°C during the day and 23.0°C at night. Relative humidity was 70% during the day and 90% at night. Broad bean (*V. faba* L. 'Komasakae') plants were grown for 6–7 weeks after being sown in pots filled with Kureha compost (KUREHA Co., Chuo, Tokyo, Japan). The plants were illuminated for 13 h each day with fluorescent lights at a PPF of 250 µmol m^{-2} s^{-1}. Air temperature was 26.0°C during the day and 22.0°C at night. Relative humidity was 60% during the day and 80% at night. Boston fern and broad bean plants were watered daily with a 1 : 1,000 dilution of HYPONeX nutrient solution (HYPONeX Japan Co., Setagaya, Tokyo, Japan). Fully expanded mature intact leaves were used for the experiments. The experiments were performed in room environments of 25°C air temperature and 60% relative humidity. Whole-leaf specimens of Boston fern plants, with a major leaf axis approximately 1–1.5 cm long, were used for CLSM investigations. For CLSM investigations of broad bean plants, leaf specimens were cut into approximately 1.5 cm squares immediately after being cut from an individual plant and were then placed immediately on a wetted cover glass. The abaxial leaf surface touching the cover glass was wetted with water, and the top surface was kept exposed to air.

Computer-aided system for 3D chlorophyll fluorescence imaging with CLSM

The computer-aided chlorophyll fluorescence imaging system with modified high-speed rotating pinhole disk (Nipkow disk) CLSM consisted of an inverted light microscope, a confocal scanner unit, a 488 nm wavelength laser diode system, two types of cooled CCD camera, various controlling devices and a personal computer. The Nipkow disk confocal scanner unit (modified version of model CSU-10, Yokogawa Electric, Co., Musashino, Tokyo, Japan) was installed between a highly sensitive cooled EM-CCD camera (C9100-12, Hamamatsu Photonics K.K., Hamamatsu, Shizuoka, Japan) and an inverted light microscope (IX-71, Olympus Co., Ltd., Shinjuku, Tokyo, Japan). A laser diode system (HPU50100-PFS-2, $\lambda = 488$ nm, Yokogawa Electric Co., Musashino, Tokyo, Japan) was used as the light source for CLSM. To remove reflected light and to measure chlorophyll fluorescence, a long-pass filter ($\lambda > 515$ nm) was built into the confocal scanner unit (Omasa and Konishi 2008).

A *z*-scan motor, which changed the position of the objective along the *z*-axis, was controlled by the motor controller (MAC 5000, Ludl Electronic Products Ltd., Hawthorone, NY, U.S.A.) with 0.1 µm accuracy. For more precise and rapid control of the objective position, a piezo *z*-scan unit (PIFOC, Physik Instruments, Waldbronn, Germany) was used. The working distance and the resolution of the piezo *z*-scan unit were 100 µm and 10 nm, respectively. Use of the piezo *z*-scan unit made it possible to capture an image of each different focal plane in 30 ms. The *z*-scan motor and the piezo *z*-scan unit were controlled with the computer. External and built-in electromagnetic shutters added to the confocal scanner unit were used for passing, blocking or dimming the laser beam through neutral density (ND) filters. Both shutters

were controlled by our own software via a shutter controller connected to the computer. The external shutter could be switched to select between the aperture and an ND filter, and the built-in shutter could be switched between aperture and no aperture. Timing of the control of the piezo *z*-scan unit, the shutters and the A/D conversion of the EM-CCD camera was synchronized. A disk rotation controller was newly added to adjust the rotation speed of the Nipkow disk and thus eliminate Moiré fringes resulting from delicate gaps in timing between the disk speed and A/D conversion.

Chlorophyll fluorescence intensity images were captured with the EM-CCD camera at resolutions of 512 horizontal × 512 vertical pixels × 14-bit gray level per frame, recorded as 16-bit digital data on the main memory in the computer, and analyzed by commercial software (MetaMorph, Molecular Devices Inc., Toronto, Canada; ERDAS IMAGINE, Leica Geosystems Geospatial Imaging LLC, Heerbrugg, Switzerland) and our own software. Transmitted light images of the leaves irradiated from above with a halogen lamp unit (U-LH100L-3, TH4-100, Olympus Co., Ltd., Shinjuku, Tokyo, Japan) were captured with a cooled color CCD camera (C5310, Hamamatsu Photonics K.K., Hamamatsu, Shizuoka, Japan). The images were recorded on the computer via a digital color video recorder (DSR-V10, Sony Co., Minato, Tokyo, Japan) at 640 horizontal × 480 vertical pixels per frame with 24-bit resolution. An immersion objective (UApo, ×40, numerical aperture: 1.35, Olympus Co., Ltd., Shinjuku, Tokyo, Japan) was used for all experiments.

Performance of computer-aided CLSM system

EM-CCD camera characteristics. The sensitivity of the EM-CCD camera, from 1 to approximately 2,000 times, was controlled from the computer by setting digital gain values at 0–255. The fluorescence intensities of a standard fluorescent sheet were measured with the computer-aided CLSM system at 30 different laser intensities and digital gain values of 50, 100 and 150 for the EM-CCD camera. The values revealed a positive linear relationship between fluorescence intensity and the A/D conversion level at each gain value for A/D conversion levels in the range 500–14,500. For this reason, we used A/D conversion levels in the range 500–14,500.

Measurement of PPF on the measuring plane through an objective. A metal pinhole disk (PA-50, Sigma Koki Co., Ltd., Sumida, Tokyo, Japan) was used to measure the PPF of the laser beam on the measuring plane (specimens or fluorescent sheet) through an objective (×40). The disk was 9.5 mm in external diameter and within 0.2 mm thick, and had one pinhole 50 µm in diameter. The measurement procedure was as follows: first, the beam exit of the glass fiber connected to the laser system was set 4 cm above the PPF sensor (LI-250, Licor Inc., Lincoln, NE, U.S.A.) to achieve adequate uniformity in the laser beam intensity on the sensor face, the diameter of which was approximately 8 mm. The PPF of the laser beam was measured through the cover glass of the specimen, which was set on top of the PPF sensor. Secondly, the metal pinhole disk was installed between the sensor and the cover glass. The 50 µm pinhole was fixed on the center of the sensor face. The PPF of the laser beam was measured through the cover glass and the pinhole. The scale factor between PPFs was derived by these first and second procedures with and without the pinhole and was calculated as 5,035 [standard error = 39 (n = 10)]. Finally, the PPF was measured on the measuring plane of the CLSM system through the objective, with the pinhole and the cover glass on the sensor unchanged. The true PPF on the measuring plane of the CLSM system was calculated by multiplying the measured PPF by the scale factor. The relationship between laser power and calculated PPF was expressed as a linear equation ($y = 11{,}311x - 833.4$, where x is the laser power (mW) and y is the calculated PPF (µmol m^{-2} s^{-1},) $R^2 = 1$).

Control and measurement of laser beam intensity for the saturation pulse method. The chlorophyll fluorescence parameters Φ_{PSII} and NPQ were calculated by the saturation pulse method, by producing a time sequence combination of darkness, actinic light and saturation light pulse on the measuring plane of the microscope, with external and built-in electromagnetic shutters added to the confocal scanner unit. The laser beam intensity required to achieve a saturation light pulse was first determined by adjustment of the laser power and the above-mentioned direct measurement method using the metal pinhole disk. The actinic light intensity was adjusted by selection of the ND filter inserted into the external electromagnetic shatter. The time course of the laser beam intensity (PPF) on the measuring plane of the microscope was estimated from changes in the fluorescence intensity of the standard fluorescent sheet, as measured with the EM-CCD camera connected to the CLSM system. The A/D conversion values of fluorescence intensity were calibrated in accordance with the PPF values of the above-mentioned direct measurements.

The electromagnetic shutters opened within 90 ms in the dark and within 60 ms under the actinic light conditions to generate the saturation light pulse under constant laser power. The shutters closed within 270 ms after the irradiation of specimens for approximately 2 s with a saturation light pulse. The actinic light and the saturation light pulse irradiated the specimens with uncertainties of −1.46 to +1.37% and −0.45 to +0.32% of the average intensities, respectively (see **Supplementary Fig. A**).

Each of the numerous pinholes on the rotating Nipkow disk built into the confocal scanner unit had a diameter of 50 µm. The pinholes were gyroidally placed on the disk 250 µm apart. The rotational frequency was set at 25–30 rounds s^{-1} to eliminate interference patterns (Moiré fringes).

The pattern of the pinhole arrangement was replaced every 30° revolution of the disk such that each point on the leaf was irradiated at 300–360 times s^{-1}. In this way, the light intensity measured with the EM-CCD and PPF sensor (LI-250, Licor Inc., Lincoln, NE, U.S.A.) was the average at the site irradiated with the laser beam at 300–360 times s^{-1}.

Confirmation of saturation light pulse intensity and duration of saturation of photosynthetic electron transport

To determine the saturation light intensity, changes in fluorescence yields were examined at different light pulse intensities for 2 s in darkness and light using the CLSM system and a conventional system. Microscopic chlorophyll fluorescence intensity images of the abaxial leaf surfaces were captured with the CLSM system (×40 objective) at different intensities of laser light pulses. To provide the flexibility necessary to allow changes in the ratio of saturation light pulse intensity to actinic light intensity, the actinic light was applied through a blue band-pass filter (470 nm < λ <495 nm, Olympus Co., Ltd., Shinjuku, Tokyo, Japan) from the halogen lamp unit instead of the 488 nm diode laser. Change overs from actinic light to laser pulses were performed by manually rotating a knob on the microscope. The leaf specimen was set on a wetted cover glass (NEO, 24 × 32 mm, Matsunami Glass Ind., Ltd., Kishiwada, Osaka, Japan) and used for the CLSM system. After the leaf specimen had been maintained in the dark for at least 20 min, it was irradiated with 300 μmol m^{-2} s^{-1} actinic light over a 30 min period before the laser pulse irradiations were started. The laser light pulses were applied for 2 s at 1 min intervals to avoid activation of the xanthophyll cycle. The mean values of chlorophyll fluorescence yield (chlorophyll fluorescence intensity/light intensity) of guard cell chloroplasts (>10) and mesophyll chloroplasts (>20) on the abaxial leaf side in response to different light pulse intensities in the dark and under actinic light were computed. The chlorophyll fluorescence intensity images from the abaxial surfaces of the same leaf specimens were then captured with a conventional chlorophyll fluorescence imaging system (Omasa and Takayama 2003), which consisted of several 180 W metal halide light sources (LS-M180, Sumita Optical Glass Inc., Urawa, Saitama, Japan), each equipped with a short-pass filter (4-96, λ <600 nm, Corning Inc., Corning, NY, U.S.A.), a heat-absorbing filter and optical fibers; and a cooled CCD camera (C5985-02, Hamamatsu Photonics K.K., Hamamatsu, Shizuoka, Japan) equipped with a long-pass filter (2-64, λ >640 nm, Corning Inc., Corning, NY, U.S.A.) Actinic light at 300 μmol m^{-2} s^{-1} and light pulses of different intensities were supplied with the metal halide lamps. The average chlorophyll fluorescence yields of the abaxial leaf surface measured with the conventional system were compared with those of guard cell chloroplasts and mesophyll chloroplasts measured with the CLSM system.

To investigate the duration of saturation of photosynthetic electron transport during saturation light irradiation, the changes in intensity of chlorophyll fluorescence for the abaxial leaf cells in response to the saturation light were measured with the CLSM system under different actinic light conditions. Before irradiation with the saturation light, leaf specimens were adapted to the dark or to actinic light at 98 or 248 μmol m^{-2} s^{-1} for at least 30 min. Saturation light and actinic light were produced with the 488 nm diode laser and the electromagnetic shutters with an ND filter providing 4.11% transmittance. This gave a saturation light intensity of 4,870 μmol m^{-2} s^{-1} for leaf specimens adapted to the dark, and a saturation light intensity 24.33 times the actinic light intensity for leaf specimens adapted to actinic light at 98 or 248 μmol m^{-2} s^{-1}.

Reconstruction of 3D chlorophyll fluorescence intensity images and calculation of chlorophyll fluorescence parameters

To calculate the chlorophyll fluorescence parameters Φ_{PSII} and NPQ by the saturation pulse method, we measured changes in the intensity of chlorophyll fluorescence images of leaf specimens by the CLMS system during a time sequence combination of dark, actinic light and saturation light pulse (see **Supplementary Fig. A**). To reconstruct the 3D-$^{i}F_{m}$ image, a series of chlorophyll fluorescence intensity images taken during saturation laser light pulses in the dark ($^{i}F_{m}$) was first captured at 64 different focal planes for 1.92 s from 0.2 s after the start of irradiation. The first focal plane was located close to the abaxial leaf surface and the last focal plane was at a depth of 80 μm in the direction of the abaxial surface. Each image was captured at 30 ms intervals (exposure time of the EM-CCD) after a 1.25 μm movement of the focal plane. Secondly, after the leaf specimen had been irradiated by the actinic laser light for 20 min, another series of chlorophyll fluorescence intensity images (^{i}F) was captured at 64 different focal planes for 0.064t s at t ms intervals (t = exposure time) to reconstruct the 3D-^{i}F image. Finally, just after the capture of ^{i}F, a final series of chlorophyll fluorescence intensity images ($^{i}F_{m}'$) taken during the saturation laser light pulse under actinic light was captured in the same way as the $^{i}F_{m}$ to reconstruct the 3D-$^{i}F_{m}'$. Dark current images were captured at both exposure times in the dark. The dark current images are represented by $^{i}D_{30}$ and $^{i}D_{t}$, and were captured when exposure times were 30 ms and t ms, respectively.

Fig. 9 shows the procedure used for 3D reconstruction and the calculation of Φ_{PSII} and NPQ. The original digital images were first processed by a 3 × 3 median filter to remove the spike noise. The 3D reconstruction was performed

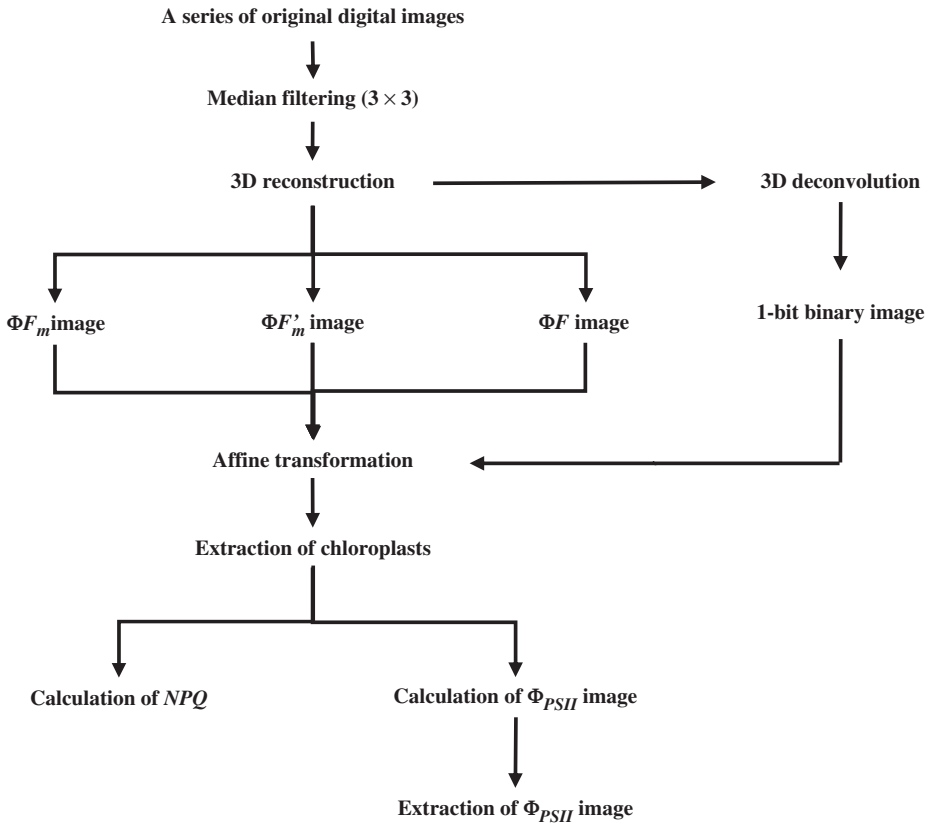

Fig. 9 Procedure used for 3D image reconstruction and calculation of Φ_{PSII} and NPQ. A series of chlorophyll fluorescence intensity images, ${}^{i}F_{m}$, ${}^{i}F_{m}'$ and ${}^{i}F$, were used for the original digital images.

with MetaMorph software to select the brightest focal plane (z coordinate) at each x–y coordinate from the 64 median-processed images measured at different focal planes. The reconstructed images were used to calculate the 3D-Φ_{PSII} image and NPQ values. These images were also deconvoluted to enhance contrast by using the nearest–neighbor method of commercially available software (AutoDeblur/AutoVisualize, AutoQuant Imaging, Inc., Troy, NY, U.S.A.)

The Φ_{PSII} images were calculated from the 3D-reconstructed, affine-transformed, and undeconvoluted ${}^{i}F$, ${}^{i}F_{m}'$, ${}^{i}D_{30}$, and ${}^{i}D_{t}$ images by the following equations, because although the deconvoluted image was clearer, the A/D conversion level of the chlorophyll fluorescence intensity was inaccurate. The symbols Φ, I and a represent yield, irradiated

$$\Phi_{PSII} = \frac{\Phi F_m' - \Phi F}{\Phi F_m'} \quad (1)$$

light intensity and the absorption coefficient of the photosynthetic pigments.

$$\Phi F_m' = \frac{\frac{1}{30} \times ({}^{i}F_m' - {}^{i}D_{30})}{24.33 \times I \times a} \quad (2)$$

$$\Phi F = \frac{\frac{1}{t} \times ({}^{i}F - {}^{i}D_t)}{I \times a} \quad (3)$$

where

The Φ_{PSII} images of chloroplasts alone were obtained by multiplying the 3D-Φ_{PSII} undeconvoluted image by a 1-bit binary image of chloroplasts extracted from the deconvoluted fluorescence image with a clearer edge for each chloroplast, and a false-color 3D-Φ_{PSII} image was displayed.

The NPQ values were calculated from 3D-reconstructed, affine-transformed and undeconvoluted ${}^{i}F_{m}$, ${}^{i}F_{m}'$, ${}^{i}D_{30}$ and ${}^{i}D_{t}$ images in accordance with the following equations.

$$NPQ = \frac{\Phi F_m - \Phi F_m'}{\Phi F_m'} \quad (4)$$

where

$$\Phi F_m = \frac{\frac{1}{30} \times ({}^{i}F_m - {}^{i}D_{30})}{24.33 \times I \times a} \quad (5)$$

For Φ_{PSII} and NPQ calculated by Equations (1) and (4), the effects of absorption by plant pigments, in the direction of the depth for 3D imaging, are canceled by including the fluorescence yields in the numerator and the denominator.

Relationships between actinic light intensity and chlorophyll fluorescence parameters of chloroplasts in mesophyll cells, guard cells and epidermal cells

To investigate the relationships between actinic light intensity and the chlorophyll fluorescence parameters of chloroplasts in mesophyll, guard and epidermal cells, 3D-$^{i}F_{m}$, 3D-$^{i}F_{m}'$, and 3D-^{i}F images were obtained at different actinic light intensities. For Boston fern leaf specimens, a series of $^{i}F_{m}$ images used to reconstruct the 3D-$^{i}F_{m}$ image was captured at a saturation light pulse of 5,950 μmol m^{-2} s^{-1} after dark adaptation for 1 h. Thereafter, the specimens were maintained under 59 μmol m^{-2} s^{-1} actinic light for 30 min and the ^{i}F images for the 3D-^{i}F image were captured. The actinic light was changed from 59 to 105, 152, 198 and 245 μmol m^{-2} s^{-1} in interval steps of 15 min, and the ^{i}F images for the 3D-^{i}F image at each actinic light intensity were captured in turn. The $^{i}F_{m}'$ images for the 3D-$^{i}F_{m}'$ images were captured during saturation light pulses of 1,430, 2,560, 3,690, 4,820 and 5,950 μmol m^{-2} s^{-1} just after the measurement of the ^{i}F images, respectively. In addition, 3D-^{i}F and 3D-$^{i}F_{m}$ images were captured in turn at 12 μmol m^{-2} s^{-1} actinic light and during a saturation light pulse of 1,430 μmol m^{-2} s^{-1} after the same periods of dark adaptation. For broad bean leaf specimens, 3D-^{i}F and 3D-$^{i}F_{m}$ images were measured only at 12,105 and 245 μmol m^{-2} s^{-1} actinic light. The procedures were similar to those of Boston fern leaf specimens. Sixteen chloroplasts within the guard cells, epidermal cells and subjacent mesophyll cells were selected from the 3D images, and the mean values and standard errors for Φ_{PSII}, NPQ and Φ_{PSII} × actinic light intensity (PPF) were calculated for each category of chloroplasts, with the exception of Boston fern epidermal cells irradiated with 12 μmol m^{-2} actinic light, for which eight chloroplasts were selected. The EM-CCD exposure time (t) for measuring ^{i}F images was 700–1,000 ms. For cells irradiated with 12 μmol m^{-2} actinic light the t value was 3,000 ms. The $\Phi F_{v}/\Phi F_{m}$ values of attached leaves were measured with a PAM 101 chlorophyll fluorimeter (Waltz).

Supplementary data

Supplementary data are available at PCP online.

Acknowledgements

We thank Mr. Hideo Hirukawa for his technical support in the development of the system. We also thank Dr. Kotaro Takayama and Dr. Ryosuke Endo for their helpful discussions.

References

Baker, N.R. and Oxborough, K. (2004) Chlorophyll fluorescence as a probe of photosynthetic productivity. *In* Chlorophyll *a* Fluorescence. A Signature of Photosynthesis. Edited by Papageorgiou,G.C. and Govindjee, pp. 65–82. Springer, Dordrecht, The Netherlands.

Baker, N.R., Oxborough, K., Lawson, T.L. and Morison, J.I.L. (2001) High resolution imaging of photosynthetic activities of tissues, cells and chloroplasts in leaves. *J. Exp. Bot.* 52: 615–621.

Bilger, W. and Björkman, O. (1990) Role of the xanthophyll cycle in photoprotection elucidated by measurements of light-induced absorbency changes, fluorescence and photosynthesis in leaves of *Hedera canariensis*. *Photosynth. Res.* 25: 173–185.

Chaerle, L., Leinonen, I., Jones, H.G. and Van Der Straeten, D. (2007) Monitoring and screening plant populations with combined thermal and chlorophyll fluorescence imaging. *J. Exp. Bot.* 58: 773–784.

Daley, P.F., Raschke, K., Ball, J.T. and Berry, J.A. (1989) Topography of photosynthetic activity of leaves obtained from video images of chlorophyll fluorescence. *Plant Physiol.* 90: 1233–1238.

Endo, R. and Omasa, K. (2004) Chlorophyll fluorescence imaging of individual algal cells: effects of herbicide on *Spirogyra distenta* at different growth stages. *Environ. Sci. Technol.* 38: 4165–4168.

Endo, R. and Omasa, K. (2007) 3-D cell-level chlorophyll fluorescence imaging of ozone-injured sunflower leaves using a new passive light-microscope system. *J. Exp. Bot.* 58: 765–772.

Evans, J.R. and Vogelmann, T.C. (2003) Profiles of C-14 fixation through spinach leaves in relation to light absorption and photosynthetic capacity. *Plant Cell Environ.* 26: 547–560.

Evans, J.R. and von Caemmerer, S. (1996) Carbon dioxide diffusion inside leaves. *Plant Physiol.* 110: 339–346.

Genty, B., Briantais, J.M. and Baker, N.R. (1989) The relationship between the quantum yield of photosynthetic electron-transport and quenching chlorophyll fluorescence. *Biochim. Biophys. Acta* 990: 87–92.

Genty, B. and Meyer, S. (1995) Quantitative mapping of leaf photosynthesis using chlorophyll fluorescence imaging. *Aust. J. Plant Physiol.* 22: 277–284.

Gilmore, A.M., Shinkarev, V.P., Hazlett, T.L. and Govindjee (1998) Quantitative analysis of the effects of intrathylakoid pH and xanthophyll cycle pigments on chlorophyll *a* fluorescence lifetime distributions and intensity in thylakoids. *Biochemistry* 37: 13582–13593.

Goh, C.-H., Schreiber, U. and Hedrich, R. (1999) New approach of monitoring changes in chlorophyll *a* fluorescence of single guard cells and protoplasts in response to physiological stimuli. *Plant Cell Environ.* 22: 1057–1070.

Govindjee (1995) Sixty-three years since Kautsky: chlorophyll *a* fluorescence. *Aust. J. Plant Physiol.* 22: 131–160.

Govindjee and Nedbal, L. (2000) Seeing is believing. *Photosynthetica* 38: 481–482.

Govindjee and Seufferheld, M.J. (2002) Non-photochemical quenching of chlorophyll *a* fluorescence: early history and characterization of two xanthophyll-cycle mutants of *Chlamydomonas reinhardtii*. *Funct. Plant Biol.* 29: 1141–1155.

Han, T., Vogelmann, T. and Nishio, J. (1999) Profiles of photosynthetic oxygen-evolution within leaves of *Spinacia oleracea*. *New Phytol.* 143: 83–92.

Ichihara, A., Tanaami, T., Isozaki, K., Sugiyama, Y., Kosugi, Y., Mikuriya, K., et al. (1996) High speed confocal fluorescence microscopy using a Nipkow scanner with microlenses for 3-D imaging of single fluorescent molecule in real-time. *Bioimages* 4: 57–62.

Koizumi, M., Takahashi, K., Mineuchi, T., Nakamura, K. and Kano, H. (1998) Light gradients and the transverse distribution of chlorophyll fluorescence in mangrove and *Camellia* leaves. *Ann. Bot.* 81: 527–533.

Kopka, J., Provart, N.J. and Müller-Röber, B. (1997) Potato guard cells respond to drying soil by a complex change in the expression of genes related to carbon metabolism and turgor regulation. *Plant J.* 11: 871–882.

Kramer, D.M., Sacksteder, C.A. and Cruz, J.A. (1999) How acidic is the lumen? *Photosynth. Res.* 60: 151–163.

Krause, G.H., Jahns, P. (2004) Non-photochemical energy dissipation determined by chlorophyll fluorescence quenching: characterization and function. *In* Chlorophyll *a* Fluorescence. A Signature of Photosynthesis. Edited by Papageorgiou, G.C. and Govindjee, pp. 463–495. Springer, Dordrecht, The Netherlands.

Küpper, H., Šetlík, I., Trtílek, M. and Nedbal, L. (2000) A microscope for two-dimensional measurements of in vivo chlorophyll fluorescence kinetics using pulsed measuring radiation, continuous actinic radiation, and saturating flashes. *Photosynthetica* 38: 553–570.

Lawson, T., Oxborough, K., Morison, J.I.L. and Baker, N.R. (2002) Responses of photosynthetic electron transport in stomatal guard cells and mesophyll cells in intact leaves to light, CO_2, and humidity. *Plant Physiol.* 128: 52–62.

Lawson, T., Oxborough, K., Morison, J.I.L. and Baker, N.R. (2003) The responses of guard and mesophyll cell photosynthesis to CO_2, O_2, light, and water stress in a range of species are similar. *J. Exp. Bot.* 54: 1743–1752.

Lazár, D. (1999) Chlorophyll *a* fluorescence induction. *Biochim. Biophys. Acta* 1412: 1–28.

Leipner, J., Oxborough, K. and Baker, N.R. (2001) Primary sites of ozone-induced perturbations of photosynthesis in leaves: identification and characterization in *Phaseolus vulgaris* using high resolution chlorophyll fluorescence imaging. *J. Exp. Bot.* 52: 1689–1696.

Lichtenthaler, H.K. and Miehé, J.A. (1997) Fluorescence imaging as a diagnostic tool for plant stress. *Trends Plant Sci.* 2: 316–320.

Minsky, M. (1988) Memoir on inventing the confocal scanning microscope. *Scanning* 10: 128–138.

Nakano, A. (2002) Spinning-disk confocal microscopy—a cutting-edge tool for imaging of membrane traffic. *Cell Struct. Funct.* 27: 349–355.

Noctor, G. and Horton, P. (1990) Uncoupler titration of energy-dependent chlorophyll fluorescence quenching and photosystem-II photochemical yield in intact pea-chloroplasts. *Biochim. Biophys. Acta* 1016: 228–234.

Omasa, K. (1998) Image instrumentation of chlorophyll *a* fluorescence. *SPIE* 3382: 91–99.

Omasa, K. (2000) 3-D color video microscopy of intact plants. *In* Image Analysis: Methods and Applications, 2nd edn. Edited by Häder, D.P. pp. 257–273 CRC Press, Boca Raton, FL.

Omasa, K., Hosoi, F. and Konishi, A. (2007) 3D lidar imaging for detecting and understanding plant responses and canopy structure. *J. Exp. Bot.* 58: 881–898.

Omasa, K., Konishi, A. (2008) Development of a 3D confocal laser scanning microscope for applying the saturation pulse method to chlorophyll a fluorescence. *In* Photosynthesis. Energy from the Sun. 14th International Congress on Photosynthesis. Edited by Allen, J.F., Gantt, E., Golbeck, J.H., and Osmond, B. pp. 657–660. Springer, Berlin.

Omasa, K., Shimazaki, K, Aiga, I., Larcher, W. and Onoe, M. (1987) Image analysis of chlorophyll fluorescence transients for diagnosing the photosynthetic system of attached leaves. *Plant Physiol.* 84: 748–752.

Omasa, K., Takayama, K. (2002) Image instrumentation of chlorophyll *a* fluorescence for diagnosing photosynthetic injury. *In* Air Pollution and Plant Biotechnology. Edited by Omasa, K., Saji, H., Youssefian, S., and Kondo, N. pp. 287–308, Springer, Tokyo.

Omasa, K. and Takayama, K. (2003) Simultaneous measurement of stomatal conductance, non-photochemical quenching, and photochemical yield of photosystem II in intact leaves by thermal and chlorophyll fluorescence imaging. *Plant Cell Physiol.* 44: 1290–1300.

Osmond, C.B. and Grace, S.C. (1994) Perspectives on photoinhibition and photorespiration in the field: quintessential inefficiencies of the light and dark reactions of photosynthesis? *J. Exp. Bot.* 46: 1351–1362.

Osmond, B., Park, Y.-M. (2002) Field-portable imaging system for measurement of chlorophyll fluorescence quenching. *In* Air Pollution and Plant Biotechnology. Edited by Omasa, K., Saji, H., Youssefian, S., and Kondo, N. pp. 309–319. Springer, Tokyo.

Osmond, B., Schwarts, O. and Gunning, B. (1999) Photoinhibitory printing on leaves, visualized by chlorophyll fluorescence imaging and confocal microscopy, is due to diminished fluorescence from grana. *Aust. J. Plant Physiol.* 26: 717–724.

Oxborough, K. (2004) Using chlorophyll a fluorescence imaging to monitor photosynthetic performance. *In* Chlorophyll *a* Fluorescence. A Signature of Photosynthesis. Edited by Papageorgiou, G.C., and Govindjee. pp. 409–428. Springer, Dordrecht, The Netherlands.

Oxborough, K. and Baker, N.R. (1997a) An instrument capable of imaging chlorophyll *a* fluorescence from intact leaves at very low irradiance and at cellular and subcellular levels of organization. *Plant Cell Environ.* 20: 1473–1483.

Oxborough, K. and Baker, N.R. (1997b) Resolving chlorophyll *a* fluorescence images of photosynthetic efficiency into photochemical and non-photochemical components—calculation of qP and Fv′/Fm′ measuring Fo′. *Photosynth. Res.* 54: 135–142.

Papageorgiou, G.C., Govindgee (eds) (2004) Chlorophyll *a* Fluorescence. A Signature of Photosynthesis. Springer, Dordrecht, The Netherlands.

Pfündel, E. and Neubohn, B. (1999) Assessing photosystem I and photosystem II distribution in leaves from C4 plants using confocal laser scanning microscopy. *Plant Cell Environ.* 22: 1569–1577.

Rigaut, J.P., Carvajal-Gonzalez, S., Vassy, J. (1992) Confocal image cytometry—quantitative analysis of three-dimensional images obtained by confocal scanning microscopy. *In* Image Analysis in Biology. Edited by Häder, D.P, pp. 109–133. CRC Press, Baca Raton, FL.

Rolfe, S.A. and Scholes, J.D. (1995) Quantitative imaging of chlorophyll fluorescence. *New Phytol.* 131: 69–79.

Rolfe, S.A. and Scholes, J.D. (2002) Extended depth-of-focus imaging of chlorophyll fluorescence from intact leaves. *Photosynth. Res.* 72: 107–115.

Schreiber, U. (2004) Pulse-amplitude-modulation (PAM) fluorometry and saturation pulse method: an overview. *In* Chlorophyll *a* Fluorescence. A Signature of Photosynthesis. Edited by Papageorgiou, G.C. and Govindgee. pp. 279–319. Springer, Dordrecht, The Netherlands.

Schurr, U., Walter, A. and Rascher, U. (2006) Functional dynamics of plant growth and photosynthesis—from steady-state to dynamics—from homogeneity to heterogeneity. *Plant Cell Environ.* 29: 340–352.

Shimazaki, K. (1989) Ribulosebisphosphate carboxylase activity and photosynthetic O_2 evolution rate in *Vicia* guard-cell protoplasts. *Plant Physiol.* 91: 459–463.

Shimazaki, K., Doi, M. Assmann, S.M. and Kinoshita, T. (2007) Light regulation of stomatal movement. *Annu. Rev. Plant Biol.* 58: 219–247.

Shimazaki, K., Gotow, K. and Kondo, N. (1982) Photosynthesis properties of guard cell protoplasts from *Vicia faba* L. *Plant Cell Physiol.* 23: 871–879.

Shimazaki, K., Gotow, K., Sakaki, T. and Kondo, N. (1983) High respiratory activity of guard cell protoplasts from *Vicia faba* L. *Plant Cell Physiol.* 24: 1049–1056.

Strasser, R.J., Tsimilli-Michael, M., Srivastava, A. (2004) and Analysis of the chlorophyll *a* fluorescence transient. *In* Chlorophyll *a* Fluorescence. A Signature of Photosynthesis. Edited by Papageorgiou, G.C.,Govindjee. 321–362. Springer, Dordrecht, The Netherlands.

Takahashi, K., Mineuchi, K., Nakamura, T., Koizumi, M. and Kano, H. (1994) A system for imaging transverse distribution of scattered light and chlorophyll fluorescence in intact rice leaves. *Plant Cell Environ.* 17: 105–110.

Tanaami, T., Otsuki, S., Tomosada, N., Kosugi, Y., Shimizu, M. and Ishida H. (2002) High-speed 1-frame/ms scanning confocal microscope with a microlens and Nipkow disks. *Appl. Opt.* 41: 4704–4708.

Terashima, I., Miyazawa, S.I. and Hanba, Y. (2001) Why are sun leaves thicker than shade leaves? Consideration based on analyses of CO_2 diffusion in the leaf. *J. Plant Res.* 114: 93–105.

Tlałka, M. and Fricker, M. (1999) The role of calcium in blue-light-dependent chloroplast movement in *Lemna trisulca* L. *Plant J.* 20: 461–473.

Tlałka, M., Runquist, M. and Fricker, M. (1999) Light perception and the role of the xanthophyll cycle in blue-light-dependent chloroplast movements in *Lemna trisulca* L. *Plant J.* 20: 447–459.

Vani, T. and Raghavendra, A.S. (1994) High mitochondrial activity but incomplete engagement of the cyanide-resistant alternative pathway in guard cell protoplasts of pea. *Plant Physiol.* 105: 1263–1268.

Vavasseur, A. and Raghavendra, A.S. (2005) Guard cell metabolism and CO_2 sensing. *New Phytol.* 165: 665–682.

Vogelmann, T.C. and Evans, J.R. (2002) Profiles of light absorption and chlorophyll within spinach leaves from chlorophyll fluorescence. *Plant Cell Environ.* 25: 1313–1323.

Wang, E., Babbey, C.M. and Dunn, K.W. (2005) Performance comparison between the high-speed Yokogawa spinning disc confocal system and single-point scanning confocal systems. *J. Microsc.* 218: 148–159.

(Received April 2, 2008; Accepted November 12, 2008)